

Do WMAP data favor neutrino mass and a coupling between Cold Dark Matter and Dark Energy ?

G. La Vacca^{1,2}, J.R. Kristiansen³, L.P.L. Colombo⁴, R. Mainini³, S. A. Bonometto^{1,2}

¹*Physics Department G. Occhialini, Milano–Bicocca University, Piazza della Scienza 3, 20126 Milano, Italy*

²*I.N.F.N., Sezione di Milano–Bicocca, Piazza della Scienza 3, 20126 Milano, Italy*

³*Institute of Theoretical Astrophysics, University of Oslo, Box 1029, 0315 Oslo, Norway*

⁴*Department of Physics & Astronomy, University of Southern California, Los Angeles, CA 90089-0484*

E-mail: lavacca@mib.infn.it, j.r.kristiansen@astro.uio.no

ABSTRACT: Within the frame of cosmologies where Dark Energy (DE) is a self-interacting scalar field, we allow for a CDM–DE coupling and non-zero neutrino masses, simultaneously. In their 0–0 version, *i.e.* in the absence of coupling and neutrino mass, these cosmologies provide an excellent fit to WMAP, SNIa and deep galaxy sample spectra, at least as good as Λ CDM. When the new degrees of freedom are open, we find that CDM–DE coupling and significant neutrino masses (~ 0.1 eV per ν species) are at least as likely as the 0–0 option and, in some cases, even statistically favoured. Results are obtained by using a Monte Carlo Markov Chain approach.

KEYWORDS: Dark energy theory, dark matter, cosmological neutrinos, neutrino properties, cosmology of theories beyond the SM,.

Contents

1. Introduction	1
2. Self-interaction potentials	3
3. CDM–DE coupling	5
4. Data and methods	8
5. Results	9
6. Summary and conclusions	14

1. Introduction

In the late 90’s Hubble diagrams of SNIa [1] became sufficiently precise to allow the unexpected conclusion that the cosmic expansion is accelerated. This agreed with fresh Cosmic Microwave Background (CMB) [2] and large scale structure (LSS) [3] data, strongly indicating that the background metric is *spatially flat*, while the matter density parameter $\Omega_{o,m} \simeq 0.27$ is much below unity. It was then natural to infer that the rest of the energy budget (up to $\Omega_o \simeq 1$) is responsible for the cosmic acceleration; dubbed Dark Energy (DE), it ought to be a smooth non-clustering component, with a state parameter close to -1.

All data available up to now can be accomodated in a cosmology where DE has a state parameter $w \equiv -1$, a model equivalent to introducing Einstein’s cosmological constant. This minimal model is dubbed Λ CDM (or cosmic concordance) cosmology. However, DE nature has yet to be properly understood.

A component with $w \equiv -1$ could be *false vacuum*. If vacuum energy does not vanish, its expected density is m_p^4 (m_p : the Planck scale), and the measured density implies a *fine tuning* $\sim 1 : 10^{124}$. But, even referring to the last phase transition, supposed to occur when the cosmic temperature was $T_{EW} \sim 100$ GeV, the fine tuning is still $\sim 1 : 10^{56}$.

The *coincidence* paradox is even more severe. If one does not want to indulge to anthropic perspectives, a vacuum energy level just allowing structure formation, and stopping the process just when it has completed, can be hardly accepted without a justification.

Alternatives to false vacuum were then proposed, aimed to avoid fine tuning and coincidence. They mostly bring new parameters to be fitted to the same data Λ CDM already fits so nicely. The hope of a substantial increment of model likelihood was however frustrated, so that no real new insight into DE physics has yet been gained in this way.

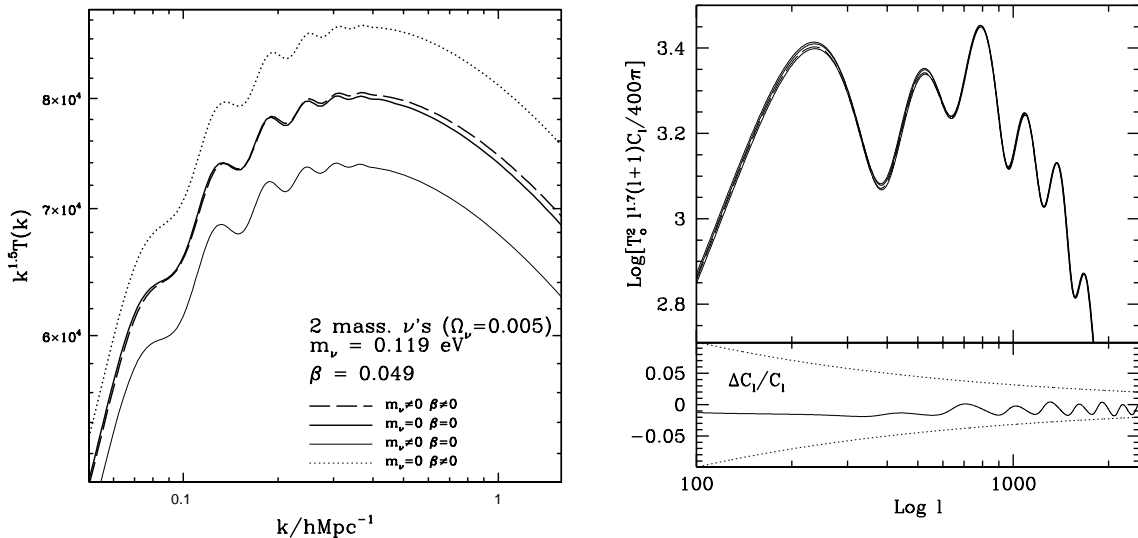


Figure 1: Transfer functions (left) and angular anisotropy spectrum (right) in cosmologies with/without coupling and with/without 2 massive ν 's (00/CM models). Coupling and mass are selected so to yield an approximate balance. The transfer functions are multiplied by $k^{1.5}$, to help the reader to distinguish different cases. In the lower frame of the C_l plot we also give the spectral differences between 00- and CM-models, hardly visible in the upper frame. Here dotted lines represent the cosmic variance interval.

A somehow alternative pattern is an unbiased fit of the scale dependence of DE state parameter $w(a)$ to data. But, although restricting to a 2-parameter expression

$$w(a) = w_o + (1 - a)w' , \quad (1.1)$$

current data hardly do more than fixing a likelihood ellipse [4], provocatorily centered on $w_o = -1, w' = 0$, and up to now, also this approach has failed to give any new insight into the DE nature.

In this paper we however keep within the latter approach, but modifying the parameter budget. We aim to test whether existing data are already more constraining, once the range of models explored is different. The option we shall explore is suggested by previous results based on a Fisher Matrix (FM) analysis [5]. Here the authors started with observing that spectral distortions due to a coupling between cold dark matter (CDM) and DE (parametrized by β , see below) or to neutrino (ν) masses are essentially opposite. This holds for both C_l and $P(k)$, the CMB anisotropy spectrum and the matter fluctuation spectrum (see Figure 1 for an example). Their FM analysis then assumes that a model with vanishing ν masses and no coupling (the 00-model) has top likelihood, and tests how far one can go, increasing ν masses and coupling, keeping within 1- σ or 2- σ from the 00-model. When a CDM-DE coupling is simultaneously allowed, they find that this allows ν masses well above the limits from the WMAP team [4], as quoted in Table 1.

In this work we shall therefore perform a full Monte Carlo Markov Chain (MCMC)

	$w = -1$	$w \neq -1$
WMAP5	$< 1.3 \text{ eV}$	$< 1.5 \text{ eV}$
WMAP5+BAO+SN	$< 0.61 \text{ eV}$	$< 0.66 \text{ eV}$

Table 1: Summary of the $2\text{-}\sigma$ (95% C.L.) constraints on the sum of ν masses [4], from WMAP 5-year, Baryonic Acoustic Oscillations and SuperNova data sets.

analysis of available data, simultaneously opening the degrees of freedom of ν mass and CDM–DE coupling.

Let us remind that CDM–DE coupling [15] eases the coincidence problem. Within Λ CDM, at $z \sim 10^3$ the DE–matter density ratio is $\sim 10^{-9}$. With coupling, instead, it could already exceed 10^{-2} . With (quasi–)vanishing ν masses, however, such coupled models clash against data, setting a limit $\beta \lesssim 0.075$ [15, 16, 17].

In turn, at least one ν mass eigenstate or, possibly, two of them exceed $\simeq 0.055 \text{ eV}$ (direct or inverse hierarchy). This follows from solar [6] and reactor [7] neutrino experiments, yielding $\Delta m_{1,2}^2 \simeq 8 \times 10^{-5} \text{ eV}^2$, and atmospheric [8] and accelerator beam [9] experiments yielding $\Delta m_{2,3}^2 \simeq 3 \times 10^{-3} \text{ eV}^2$. However, the neutrino oscillation experiments do not provide us with any information on the absolute scale of ν masses.

Cosmology is sensitive to ν masses. Already in 1984 Valdarnini & Bonometto [10] derived the transfer function for mixed DM models, with DM partially made of massive ν 's. Mixed models were widely tested in the Nineties. ν 's then filled the apparently unescapable gap between Ω_{om} and Ω_o . That gap is now neatly defined and filled by DE, as already outlined. But ν 's becoming non-relativistic cause so strong spectral distortions that even a small contribution to the density budget from them can be tested (for a thorough review on effects of massive ν 's on cosmological observables, see [11]). This gives the cosmological limits on the absolute scale of ν masses in Table 1, an order of magnitude more stringent than limits from tritium β –decay experiments.

The ambitious aim of this paper is then to show that, as both limits can be substantially relaxed, (mildly–)mixed coupled models could really be an alternative to the minimal Λ CDM cosmology with the advantage of easing both fine tuning and coincidence paradox.

The plan of the paper is as follows: In Section 2 we outline the expressions and potentials related to the interacting CDM–DE fluid. In Section 3 we review coupled DE (cDE). The data sets and statistically methods used are presented in Section 4. In Section 5 we present our results. Finally we summarize our findings and conclude in Section 6.

2. Self–interaction potentials

We shall assume that DE is a scalar field ϕ , self–interacting through the potentials

$$V(\phi) = \Lambda^{\alpha+4}/\phi^\alpha \quad RP$$

or

$$V(\phi) = (\Lambda^{\alpha+4}/\phi^\alpha) \exp(4\pi \phi^2/m_p^2) \quad SUGRA$$

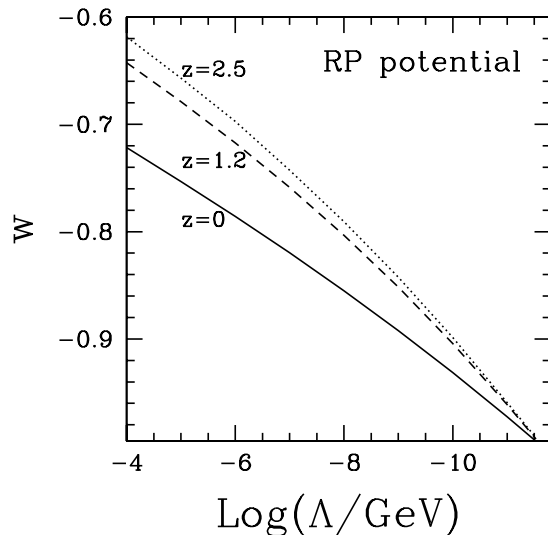


Figure 2: State parameter and its variation in uncoupled RP models. The plot is for $h = 0.7$, $\Omega_b = 0.046$, $\Omega_c = 0.209$.

admitting tracker solutions. Uncoupled RP [12] yields a slowly varying $w(a)$ state parameter, steadily below -0.85 for $\Lambda/\text{GeV} \lesssim 10^{-9}$ (see Figure 2). On the contrary, uncoupled SUGRA [13] yields a fastly varying $w(a)$, even faster than any expression (1.1), as is shown in Figure 3. Coupling is however an essential feature that we shall be considering and, in the next Section, we shall see how it modifies these behaviors.

Independently of the presence of coupling, for any choice of Λ and α these potentials yield a precise DE density parameter Ω_{de} . Here we use Λ and Ω_{de} as free parameters; the related α value is then suitably fixed.

Both RP and SUGRA potentials were initially introduced to ease the fine tuning problem. In fact, the present DE density can be tuned on today's CMB temperature T_o , reading $\rho_{o,de} \sim (10T_o)^4$; tracker solutions then require a present DE field $\phi_o \sim m_p$ so that an approximation $V(\phi_o) \sim \rho_{o,de}$ yields $m_p^\alpha (10T_o)^4 \sim \Lambda^{4+\alpha}$. For reasonable α 's, Λ is therefore of the order of the energy scale of SUSY breaking or EW transition.

Fits to data however show that uncoupled RP fails to meet CMB anisotropy data, unless the energy scale Λ stands below $\sim 10^{-9}\text{GeV}$ [14] (previous approximate relations indicate then $\alpha \sim 0.5$); this is coherent with the fact that $w(a)$ is then steadily below -0.85 ($\sim 95\%$ C.L.) as established in [4] for constant $w(a)$.

In the case of uncoupled SUGRA, however, while the best fit still leads to low Λ 's, a value $\Lambda \sim \mathcal{O}(0.1\text{GeV})$ is within $\sim 2\sigma$'s from the best-fit model. Let alone the SUSY and EW scale, this is still an energy close to the confinement scale. Coupling however causes quantitative modifications to these behaviors, that we shall see in the next Sections.

Quite in general, however, the very fact that the natural representation to describe DE is not the one where particle numbers are diagonal, is related to the smallness of the mass of the quanta. Such low particle masses, although being a natural consequence of the potential expressions, are considered a hidden fine-tuning by some researchers.

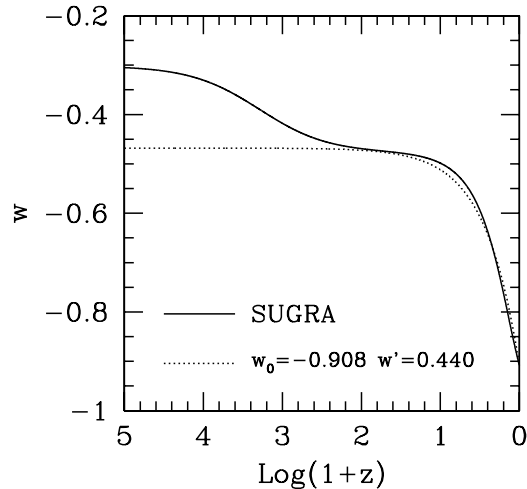


Figure 3: State parameter in models with $w(a)$ given by eq. (1.1) and in a uncoupled SUGRA model with $\Lambda = 0.1 \text{ GeV}$. w_0 and w' values (in the frame) selected to yield a behavior close to SUGRA, by requiring similar high- z plateau and $w(0)$. Although renouncing to a full coincidence at $z = 0$, the fast variability of $w(a)$ in uncoupled SUGRA cannot be met by any polynomial $w(a)$. The plot is for $h = 0.7$, $\Omega_b = 0.046$, $\Omega_c = 0.209$.

3. CDM–DE coupling

In the cDE scenario, as for dynamical DE, the scalar field ϕ yields a cosmic component unsuitable to clustering and showing a negative pressure in the present epoch. Its energy density and pressure however read

$$\rho = \rho_k + V(\phi) , \quad p = \rho_k - V(\phi) , \quad \text{with } \rho_k = \dot{\phi}^2/2a^2 ; \quad (3.1)$$

dots indicate differentiation in respect to τ (conformal time), the background metrics being

$$ds^2 = a^2(\tau) [d\tau^2 - d\lambda^2] \quad \text{with } d\lambda^2 = dr^2 + r^2(d\theta^2 + \cos^2\theta d\phi^2) . \quad (3.2)$$

These expressions show that two regimes are possible. If $\rho_k \gg V$, the DE state parameter approaches $+1$ (*stiff matter*) so that DE energy density rapidly dilutes during expansion ($\rho \propto a^{-6}$). In the opposite case $V \gg \rho_k$, the state parameter approaches -1 and DE is suitable to explain the observed cosmic acceleration.

Let us now consider the possibility that DE is coupled to other components. Interactions with baryons, constrained by observational limits on violations of the equivalence principle (see, *e.g.* [18]), are almost fully excluded. Similar constraints, however, do not exist for DE–CDM interactions. The only constraints then derive from cosmological data.

The simplest possible coupling is a linear one. It can be formally obtained by performing a conformal transformation of Brans–Dicke theory (see, *e.g.*, [19]), where gravity is modified by adding a ϕR term to the GR Lagrangian (R : Ricci scalar). Coupling causes an energy transfer between CDM and DE, so allowing DE to have a non-negligible density

even when its state parameter is $\sim +1$. However, ρ_k being then dominant, the transferred energy is soon diluted.

A so-called ϕ -matter dominated period then occurs when, because of the power leaking towards DE, CDM density declines more rapidly than a^{-3} . The increase of ϕ then brings it to approach m_p and $V(\phi)$ to exceed ρ_k . DE dilution then stops and DE eventually exceeds DM density.

The overall picture is however quite natural. All tenable cosmological models do require a dark sector, split into two components with different state equations. The fact that their interactions with baryonic matter is just gravitational, leads to requiring that

$$T^{(c)\ \mu}_{\ \nu;\mu} + T^{(de)\ \mu}_{\ \nu;\mu} = 0 \quad (3.3)$$

(here $T_{\mu\nu}^{(c,de)}$ are the stress-energy tensors of CDM and DE, let their traces read $T^{(c,de)}$), while the assumption that CDM and DE are two separate fluids leads to take $C \equiv 0$ in the relations

$$T^{(de)\ \mu}_{\ \nu;\mu} = +CT^{(c)}\phi_{,\nu} \quad (3.4)$$

$$T^{(c)\ \mu}_{\ \nu;\mu} = -CT^{(c)}\phi_{,\nu} \ , \quad (3.5)$$

describing the most general form of linear coupling (incidentally, this shows why DE cannot be linearly coupled to any component with vanishing stress-energy tensor trace).

Assuming two separate fluids is clearly an extra assumption and, if we allow for $C \neq 0$, when the metric is (3.2), these equations yield

$$\ddot{\phi} + 2\frac{\dot{a}}{a}\dot{\phi} + a^2V'_\phi = +Ca^2\rho_c \quad (3.6)$$

$$\dot{\rho}_c + 3\frac{\dot{a}}{a}\rho_c = -C\rho_c\dot{\phi} \quad (3.7)$$

ρ_c being CDM energy density.

General covariance requires C to be a constant or to evolve as a function of ϕ itself. Here, instead of C , we shall mostly use the adimensional parameter

$$\beta = (3/16\pi)^{1/2}m_p C \quad (3.8)$$

and consider constant β values $\mathcal{O}(0.1)$ (corresponding to $C \sim 1/2m_p$) which, as we shall see, meet observational data.

The above dynamics naturally causes a $w(a)$ behavior significantly different from the uncoupled case. In Figure 4 we plot the z dependence of the DE state parameter for the SUGRA potential. For the sake of comparison the uncoupled behavior is also shown.

In the Figure, the transition from a *stiff-matter* behavior to $w \sim -1$ is clearly shown. Such transition is later for greater coupling. At low z , for low β 's, the uncoupled behavior is reapproached and, for β as low as 0.05, the dependence of w on z , when approaching $z = 0$, is even steeper than in the uncoupled case. For greater couplings, however, the behavior gradually softens and, for $\beta \simeq 0.1$, the effective value of w at low z is systematically closer to Λ CDM than in the uncoupled case.

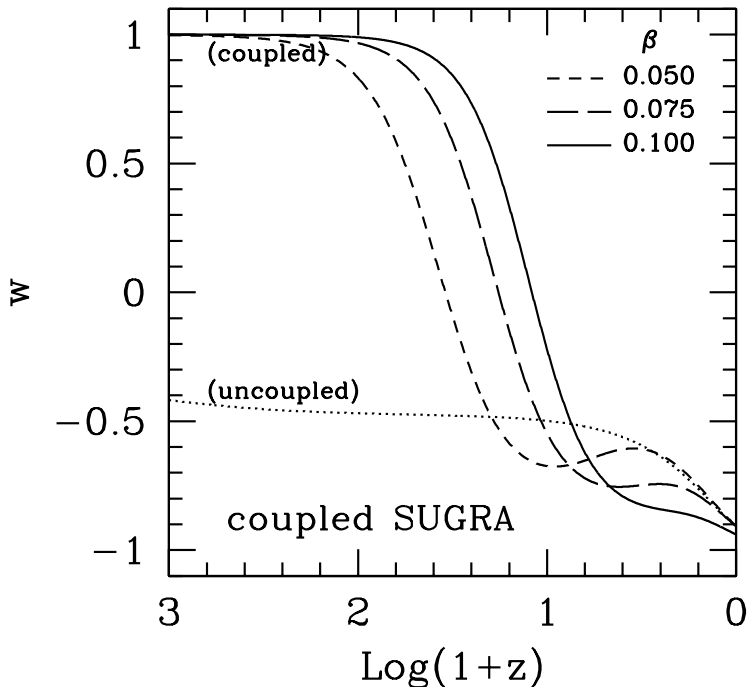


Figure 4: State parameter in coupled SUGRA model with $\Lambda = 0.1$ GeV, $h = 0.7$, $\Omega_b = 0.046$, $\Omega_c = 0.209$, as in Figure 3. The uncoupled behavior given there is reported also here.

Figure 4 also shows that the scale dependence of the state parameter exhibits a peculiar feature, even in the presence of mild couplings (*e.g.*, for $\beta = 0.05$), shifting from negative to positive values in a potentially observable redshift range. This behavior is not restricted to SUGRA potentials; it holds for RP and other potentials as well. Even approximate measurements of the scale dependence of the state parameter, extending up to $z \sim 10$ – 30 , should therefore be able to set direct limits to the coupling intensity.

The behaviors are qualitatively similar in the case of a RP potential. Figure 5, similar to Figure 2, includes a coupling $\beta = 0.1$. It shows, first of all, that w still keeps fairly constant values. Furthermore, at low z , the state parameter w is not necessarily increasing with z , as it may occur also for the SUGRA potential and is shown in Figure 4 (for $\Lambda = 10^{-1}$ GeV), *e.g.* when $\beta = 0.05$. As for SUGRA, at low z , $w(a)$ is mostly smaller in the presence of coupling. The $w = -0.85$ limit is bypassed here around $\Lambda = 10^{-5}$ GeV. We therefore expect that a fit of coupled RP with data will be already fair for Λ values greater and physically more significant.

Before concluding this Section, it may be worth defining the coupling function $f(\phi)$, through the relation

$$C(\phi) = \frac{d \log f}{d\phi} \quad (3.9)$$

so that CDM energy density scales according to

$$\rho_c(a) = \rho_{o,c}(a_o/a)^3 f(\phi) . \quad (3.10)$$

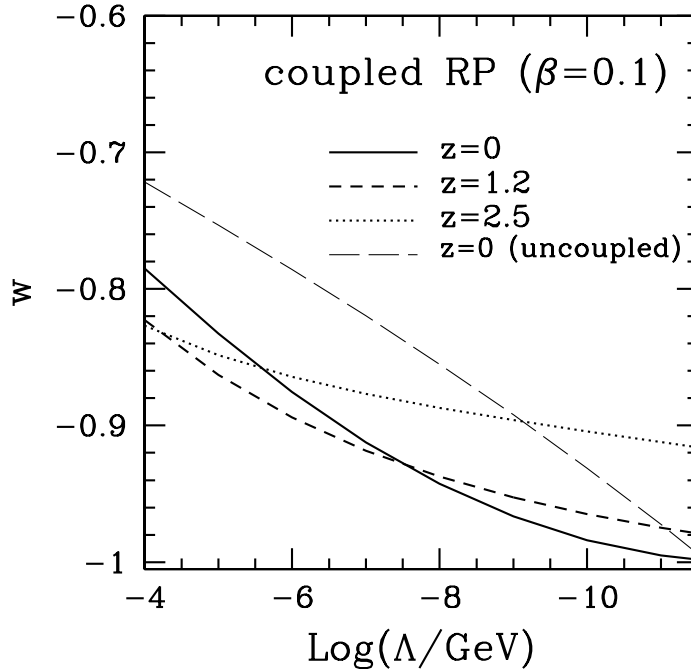


Figure 5: State parameter in coupled RP for various Λ values, in the case $\beta = 0.1$. Here $h = 0.7$, $\Omega_b = 0.046$, $\Omega_c = 0.209$, as in Figure 2. The uncoupled behavior at $z = 0$ given there is reported also here.

Then, if we set $\bar{V} = V + \rho_c$, the ϕ eq. of motion takes the (standard) form,

$$\ddot{\phi} + 2\frac{\dot{a}}{a}\dot{\phi} + a^2\bar{V}'_{\phi} = 0, \quad (3.11)$$

as though CDM and DE were decoupled, once the *effective* potential \bar{V} is used.

The CDM evolution (3.10) is then faster than in the absence of coupling. In turn, the effective behavior, obtainable by using the potential \bar{V} , mimics a *phantom*-like state equation, yielding a DE density increase with a , as we would find for $w < -1$.

This makes reasonable that neutrino mass limits are relaxed in a cDE context, as they are in the presence of phantom DE. This option, however, does not lead to requiring unconventional physics. On the contrary, by assuming quite a general behavior within the dark sector and adding the ingredient of ν mass, if we are naturally led to high β values, this will also ease the coincidence problem.

4. Data and methods

In this Section we present data sets and methods applied in our analysis.

To constrain the CMB power spectra, we use the 5 year data from the WMAP satellite [20] (WMAP5). We use both temperature and polarization data, and calculate the

likelihood of our models using the Fortran 90 code provided by the WMAP team¹.

For the matter power spectrum, we use the results from the 2dF galaxy redshift survey [21]. Constraints on the recent expansion history of the Universe is also given by the SN1a observations from the Supernova Legacy Survey (SNLS) [22].

In some cases we also apply additional priors on the Hubble parameter and the baryon density of the Universe. The prior on the Hubble parameter of $h = 0.72 \pm 0.08$ is taken from the Hubble Space Telescope (HST) Key Project [23]. Analysis of the Big Bang Nucleosynthesis [24] gives a prior on the baryon content of $\Omega_b h^2 = 0.022 \pm 0.002$.

Using many data sets will of course give stronger parameter constraints, but every additional data set might also introduce new systematics. Accordingly, we considered three different combinations of data sets in our analysis; (i) WMAP5 data only, (ii) WMAP + 2dF, (iii) WMAP + 2dF + SNLS + HST and BBN priors (henceforth named “all data”).

For the MCMC analysis we use the publicly available code CosmoMC [25] which, in turn, uses theoretical power spectra computed by a modified version of CAMB [26]. CMB lensing effects are included, to ensure accurate results when comparing with CMB polarization data. In the MCMC analysis we use the following set of basic parameters: $\{ \omega_b, \omega_c, \theta, \tau, n_s, \ln 10^{10} A_s, \Lambda, \beta, M_\nu \}$. Here: $\omega_{b,c}$ are the physical baryon and cold dark matter density parameters, $\omega_{b,c} = \Omega_{b,c} h^2$, where h is the dimensionless Hubble parameter; θ is the ratio of the sound horizon to the angular diameter distance at recombination; τ is the optical depth to reionization; n_s is the scalar spectral index; A_s denotes the amplitude of the scalar fluctuations at a scale of $k = 0.002 \text{Mpc}^{-1}$. In addition we include the sum of ν masses, $M_\nu = \Sigma m_\nu$, assuming 3 equal mass ν 's. Let us outline that Λ denotes the energy scale in DE potentials, while β is the coupling parameter between CDM and DE.

All parameters in the braces are given flat priors, unless otherwise is stated explicitly. In our MCMC analysis we also marginalize over the Sunyaev Zel'dovich amplitude, as is also done by the WMAP team in their analysis. We assume that the Universe is spatially flat. The chains are run on the Titan cluster at the University of Oslo.

In addition to MCMC runs with the full parameter set presented above, we have also repeated the analysis without M_ν or without Λ and β , to be able to compare the effects of the different extensions of the parameter space.

5. Results

In this Section we shall discuss the results of the above MCMC runs. In the cases already considered in the literature, we reobtain standard results and likelihood \mathcal{L} values. In Table 2 we report best fit values and $1-\sigma$ errors for different models.

When including the β , Λ and M_ν degrees of freedom we see that all the other parameters stay within 1σ shifts from their previous mean values. As could be expected, the error bars increase on some of the parameters, especially ω_c .

The most intriguing part of our outputs however concerns M_ν and β . Already from Table 2 one appreciates that the upper limit on ν masses has doubled. This can also be seen

¹<http://lambda.gsfc.nasa.gov>; version v3

Parameter	Λ CDM + ν 's		$w = \text{const.}$	cRP + ν 's	cSUGRA + ν 's
	WMAP only	all data	all data	all data	all data
$10^2 \omega_b$	2.244 ± 0.066	2.258 ± 0.061	2.247 ± 0.062	2.260 ± 0.061	2.260 ± 0.065
ω_c	0.1156 ± 0.0078	0.1098 ± 0.0040	0.1132 ± 0.0069	0.1039 ± 0.0062	0.1042 ± 0.0084
$10^2 \theta$	1.0401 ± 0.0030	1.0401 ± 0.0030	1.0402 ± 0.0030	1.0401 ± 0.0029	1.0406 ± 0.0030
τ	0.085 ± 0.017	0.087 ± 0.017	0.085 ± 0.017	0.087 ± 0.016	0.088 ± 0.017
M_ν (eV) (95% C.L.)	< 1.20	< 0.66	< 0.94	< 1.13	< 1.17
β (95% C.L.)	—	—	—	< 0.17	< 0.18
$\log_{10}(\Lambda/\text{GeV})$ (95% C.L.)	—	—	—	< -4.2	< 6.3
n_s	0.955 ± 0.017	0.962 ± 0.014	0.958 ± 0.015	0.969 ± 0.015	0.970 ± 0.018
$\ln(10^{10} A_s)$	3.053 ± 0.043	3.045 ± 0.040	3.049 ± 0.040	3.055 ± 0.040	3.057 ± 0.041
σ_8	0.691 ± 0.075	0.713 ± 0.056	0.711 ± 0.059	0.723 ± 0.062	0.717 ± 0.069
H_o (km/s/Mpc)	67.0 ± 4.4	70.1 ± 2.1	69.7 ± 2.2	71.8 ± 2.5	71.9 ± 2.7
$-2 \ln(\mathcal{L})$	1329.39	1407.25	1407.38	1407.44	1407.33

Table 2: Best fit values and 1- σ error bars. In all fits we allow for ν masses. The first 9 lines concern primary parameters. Only upper limits on M_ν , β and Λ are shown. These variables are discussed more thoroughly in forthcoming 2-D plots. Likelihood values are almost model independent.

in the Figures 6 and 7, where we show marginalized and average likelihood distributions on the most specific parameters of this work: β , $\log(\Lambda/\text{GeV})$ and M_ν .

Figures from the top to the bottom line refer to fits based on increasingly wide data samples. Taking WMAP5 data only, the marginalized likelihood distribution gives just a 95% C.L. upper limit $\beta < 0.28$ and $\beta < 0.23$ for SUGRA and RP potentials, respectively. When low- z data are simultaneously considered, the marginalized likelihood distributions exhibit significant maxima, which could be naively interpreted as a $\sim 2\sigma$ detection of β . A physical reason of the effect can be found in the actual tension between ω_c mean values, obtained from pure WMAP data or including low- z data, visible also in Table 2. A significant DE amount at high z could reduce there the required value of ω_c by 1-2%, and set it within 1σ from its all-data value.

In turn, models with β are somehow more likely, although one must be cautious on this point, where non-Gaussian behaviors become important, in the presence however of tiny signals. It is true, in fact, that the peak of the marginalized likelihood, in some cases, exceeds 0-0 models by almost 2σ 's. But the peak is not so pronounced among average likelihood values: here the top value is atmost double, in respect to 0-0 models. Finally, if we consider the top overall likelihood, it does not exceed Λ CDM likelihood. This seems to conflict with the fact that the likelihood of 0-0 models in RP and SUGRA cosmologies equals the likelihood of $w = -1$, among $w = \text{const}$ cosmologies. But, of course, the likelihood of individual models can easily behave differently from averaged likelihoods.

As far as the Λ scale is concerned, the $2\text{-}\sigma$ upper limit on $\log_{10}\Lambda$ is much softened compared to studies of uncoupled models. The usual upper limit $\sim 0.1\text{ GeV}$, for SUGRA models, shifts now above 10^6 GeV . Something similar occurs for the scale Λ in RP models, which is now consistent with data, within $\sim 2\sigma$'s, up to $\sim 10^{-4}\text{ GeV}$. This had been somehow predicted from Figure 5, as outlined there.

Finally, in the M_ν distributions, the gray line shows the distributions in the absence of coupling, and allows to appreciate why the 95% upper limits in Table 2 have almost doubled. The maxima in the likelihood distributions are far less accentuated here, than for β . They are somehow stronger in the SUGRA than in the RP case. It is however clear that there is no hint of ν -mass detection in these plots.

In all these plots there are discrepancies between average and marginalized likelihood distributions. They are particularly relevant as far as β is concerned.

Such discrepancies, first of all, are a safe indication of non-Gaussian distributions. In the case of β they can be better understood in association with some Figure herebelow, and they are surely the basic reason to cast serious doubts on the formal β detection from the marginalized likelihoods. The non-Gaussian behavior is minimal for ν masses.

The most significant plots of this paper are Figures 8 and 9, concerning the SUGRA and RP potentials, respectively. In these Figures, curves yield 1- and 2- σ contours for marginalized likelihood distributions. On the contrary, colors yield average likelihood distributions. The plots concern the β - M_ν and the β - $\log_{10}(\Lambda/\text{GeV})$ planes.

These plots allow, first of all, a better understanding of the discrepancy between mean and marginalized likelihood distributions. Let us consider the correlations between β and $\log_{10}(\Lambda/\text{GeV})$, shown in the lower panels. They indicate that the same β values are consis-

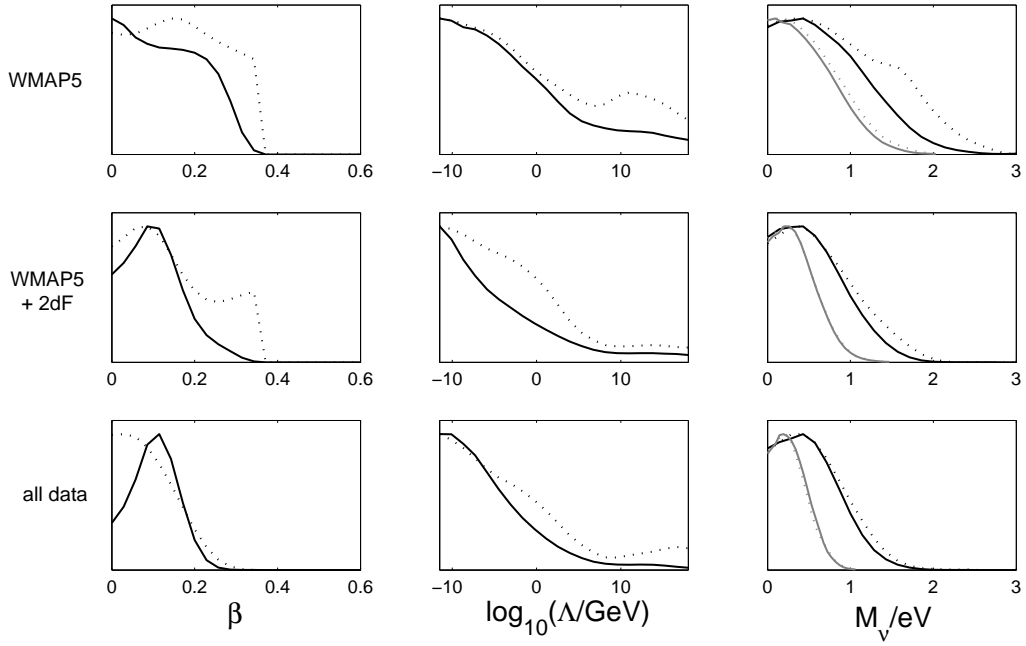


Figure 6: Marginalized (solid black line) and average (dotted black line) likelihood of cosmological parameters in SUGRA models. For M_ν we also show the corresponding likelihood distributions obtained in the case of a standard Λ CDM+ M_ν model (gray lines).

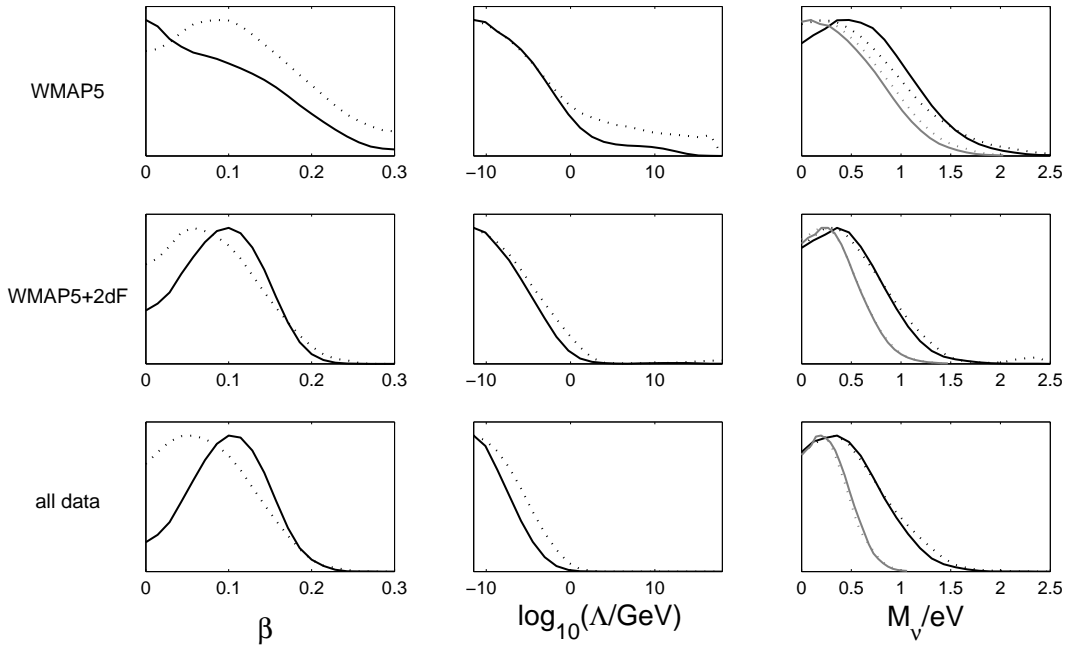


Figure 7: Marginalized (solid line) and average (dotted line) likelihood of cosmological parameters in RP models, taking into account the whole set of available data.

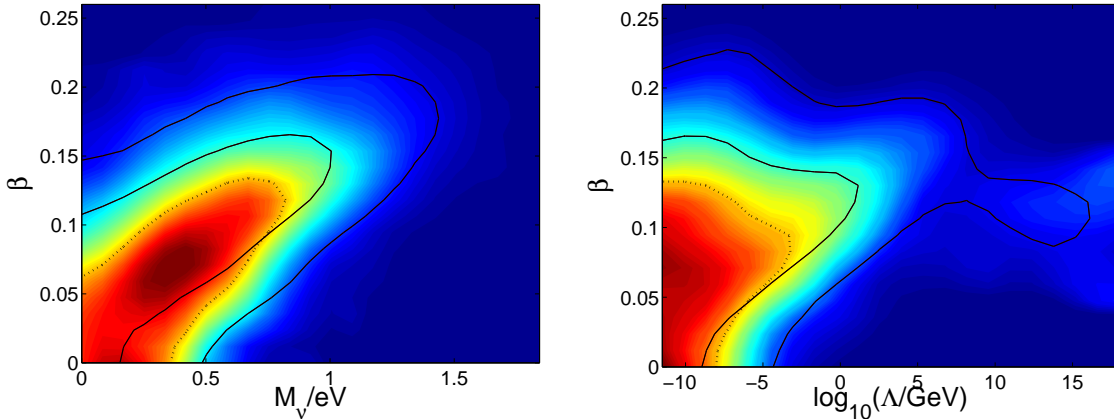


Figure 8: Two parameter contours for the SUGRA model. Solid lines are 1- and 2- σ limits for marginalized likelihood. Colors refer to average likelihood, and the 50% likelihood contour from the average likelihood is indicated by the dotted line.

tent with a fair range of Λ 's. When marginalizing over the other parameters, Λ included, this increases the weight of high β values.

In particular, Figure 8 exhibits a peculiar high- Λ tail: these 2-D plots show that, for suitable couplings $\beta \sim 0.1$, models with Λ up to 10^{15} GeV (close to GUT) are allowed within 2- σ 's. No such features is present for the RP potential. Again, however, one appreciates that $\Lambda \sim \text{MeV}$ is now allowed for RP if $\beta \sim 0.15\text{--}0.17$.

Thus, when it comes to the fine-tuning paradox, the SUGRA potential keeps a more satisfying solution than the RP potential, as a Λ scale close to the EW scale or to the scale of the soft SUSY break is consistent with data. Also RP, however, does no longer yield just unacceptably low energy scales.

One should however also consider these potentials independently of the supposedly underlying physics, as examples of rapidly or slowly varying $w(a)$. Using such potentials we could actually inspect the behaviors within these extremes, making recourse to a single parameter Λ , instead of using, *e.g.*, the parametrization $w_o\text{--}w'$, which requires 2 independent variables.

Let us then point out that, in the RP case, closer to $w = \text{const.}$, both the marginalized and the average likelihood distributions on β exhibit a maximum.

Also in the left panel of Figure 9 the likelihood peak is quite far away from $\beta = 0$, $M_\nu = 0$. In the marginalized likelihood distribution, such model is within the 95% C.L..

More in general, from the left panels of Figures 8 and 9, showing the 2D likelihood distributions in the $\beta\text{--}M_\nu$ plane, we want to stress the following points:

- (i) The solid curves in the SUGRA case substantially overlap FM results from [5] in the SUGRA case.
- (ii) Marginalized and average likelihood are different, as is expected in the presence of a non-Gaussian behavior, but not significantly so.
- (iii) Top likelihood models are found for non-vanishing β and M_ν ; the best fit values are $\beta \sim 0.07$ and $M_\nu \sim 0.35 \text{ eV}$ for both potentials.

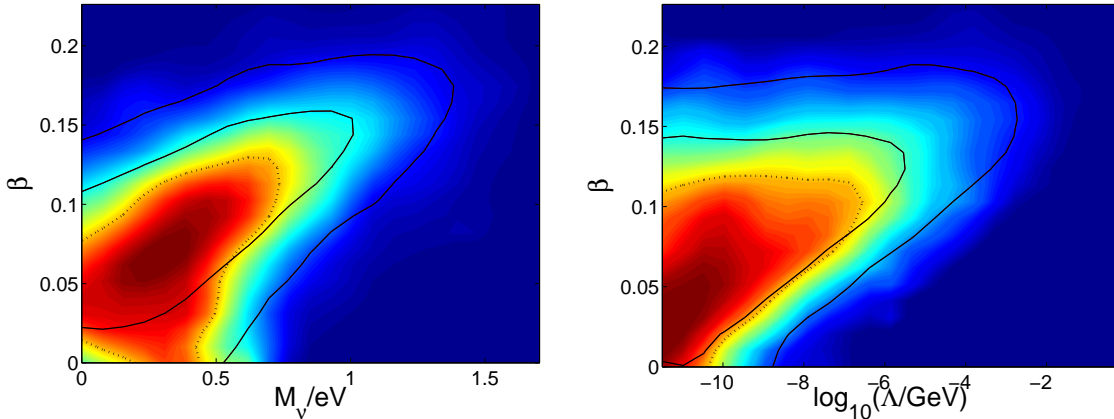


Figure 9: As previous Figure, for a RP potential.

(iv) Models with β up to 0.2 and M_ν up to 1.4 are allowed with both potentials within the 95 % C.L. . Again a result apparently potential independent.

(v) The limits on β and M_ν are strongly correlated, as expected from the FM analysis [5].

(vi) According to the marginalized likelihood distributions, $\beta = M_\nu = 0$ models are allowed for both potentials. In the RP case, however, they lay outside the $1\text{-}\sigma$ limits.

(vii) The fact that upper limits on ν masses are loosened by almost a factor 2 arises from the degeneracy between β and M_ν .

This confirms the results from [5] and shows that one should be cautious when extracting neutrino mass limits from cosmological observations, as they can heavily depend on the assumed model range, as is the case here.

6. Summary and conclusions

One of the major discoveries of physical cosmology is the existence of the dark sector of the Universe. Particles belonging to the *standard model* of elementary interactions account for not more than 5 % of its energy budget. Observations then go farther and show that the remaining 95 %, which interacts with standard model particles just through gravity, is not a single component, but needs to be modeled at least through two independent fluids, with drastically different state equations.

All existing data can be accommodated in a scheme assuming no energy exchange between these two dark components. This is simple, but leads to the well known *fine tuning* and *coincidence* paradoxes.

In this work we have explored the option that, in the dark sector, energy exchanges occur and may be described through a linear and constant coupling. Clearly, this is just the next approximation beyond assuming zero exchange and is however a phenomenological approach. Hopefully, it may lead to constraints helping to single out a precise theory, just as is done when the expression (1.1) is taken for the state parameter scale dependence.

Such option was already explored in the past. The limits found for the CDM–DE coupling were then rather deceiving. For β 's large enough, the coincidence paradox could

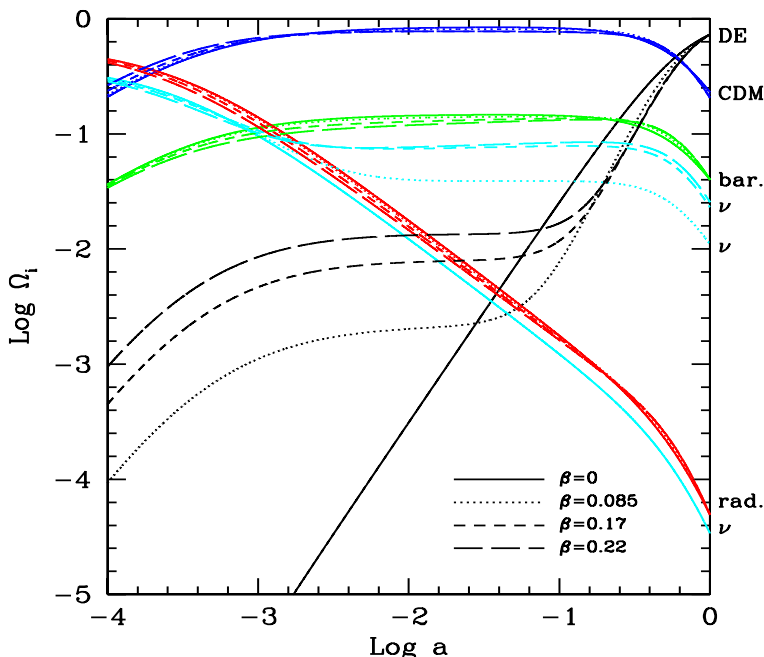


Figure 10: Evolution of the density parameters in a SUGRA model with coupling and ν mass. Colors refer to different components, as specified in the frame; lines to the different models: $M_\nu=0$, $\beta = 0$ (continuous line); $M_\nu=0.5$ eV, $\beta = 0.085$ (dotted line); $M_\nu=1.1$ eV, $\beta = 0.17$ (short dashed line); $M_\nu=1.2$ eV, $\beta = 0.22$ (long dashed line).

be significantly attenuated; but the allowed β range did not allow to go so far in this direction.

The critical ingredient of this work amounts to considering simultaneously coupling and ν masses. Massive ν 's would be a further component of the dark side, but unlike from CDM and DE, however, they are particles already known from the standard model. Furthermore, their role appears unessential to the formation of cosmic structures, although their mass can actually modify the matter distribution over the largest scales.

When one allows simultaneously ν mass and β , we find models with significantly higher likelihood. The upper limits on both parameters are softened and increase by an essential factor ~ 2 . This is a critical factor in both fields. The new allowed M_ν values approach the ν -mass detection area in forthcoming tritium decay experiments like KATRIN [27]. Moreover, when considering an external prior on M_ν from earth-based experiments, the strong degeneracy between the coupling parameter β and the neutrino mass M_ν can be broken, gaining new insight into the DE nature [28].

Simultaneously, the new allowed β values open the possibility of a critically modified DE behavior. In Figure 10 we show the scale dependence of the cosmic components for various β - M_ν pairs. They tell us that models are allowed, within the 95% C.L., for which DE is still $\sim 1\%$ of the cosmic energy budget up to $z \sim 10^3$; at higher redshifts it decreases just because the photon-neutrino fraction increases, while we approach matter-radiation equality. Such fraction attains 2-3% for the most coupled case we considered in Fig. 10,

corresponding to $C = 0.9/m_p$ with $M_\nu=1.2$ eV; this is at 2.3σ 's from the best fit. Let us remind that Λ CDM cosmologies prescribe that, at $z \sim 10^3$, DE bears less than $1 : 10^9$ of the total energy density.

Available data do not yet force us to require a non-vanishing CDM-DE coupling. The statistical analysis of data still leads to an intricate situation, where marginalized and average likelihoods exhibit discrepancies. Furthermore, the likelihood distributions on the coupling β exhibits some dependence on the selected self-interaction potential. Using a RP potential, the 0-0 option appears rather unlikely, both through marginalized and average likelihood distributions. A SUGRA potential, instead, yields a higher likelihood for the 0-0 option. Accordingly, we believe that current data do not allow a claim of " β -detection", while they certainly allow to put upper limits to the coupling, which can be so large, within the 95% C.L., to yield $C = 1/2m_p$.

Furthermore, it is fascinating to notice that, if shortly forthcoming particle data will set a lower limit to M_ν , in the range they are allowed to explore, this will imply an almost model independent CDM-DE coupling detection, opening the way to a deeper understanding of the dark sector of the Universe.

Acknowledgments

JRK and RM acknowledge financial support from the Research Council of Norway. LPLC was supported by NASA grant NNX07AH59G for this work.

References

- [1] Phillips M.M. *et al.* A.J. **104**, 1543 (1992); A. G. Riess, R. P. Kirshner, B. P. Schmidt, S. Jha, *et al.*, *Astrophys. J.***116**, 1009 (1998); S. Perlmutter, G. Aldering, G. Goldhaber, *et al.*, *Astrophys. J.***517**, 565 (1999); *then see also, e.g.* A. G. Riess, L.G. Strolger, J. Tonry, *et al.*, *Astrophys. J.***607**, 665 (2004), A.C. Becker *et al.*, arXiv:0811.4424 (astro-ph, 2008).
- [2] P. de Bernardis, P. Ade, J. Bock, *et al.*, *Nat.* **404**, 955 (2000); S. Padin, J. Cartwright, B. Mason, *et al.*, *Astrophys. J.***549**, L1 (2001); J. Kovac, E. Leitch, C. Pryke, *et al.*, *Nat.* **420**, 772 (2002); P. Scott, P. Carreira, K. Cleary, *et al.*, *Mon. Not. R. Aston. Soc.***341**, 1076 (2003); D. Spergel, R. Bean, Dorè *et al.*, *Astrophys. J.Suppl.* **170**, 377 (2007).
- [3] M. Colless, G. Dalton, S. Maddox, *et al.*, *Mon. Not. R. Aston. Soc.***329**, 1039 (2001); M. Colless, B. Peterson, C. Jackson, *et al.*, Preprint astro-ph/0306581; J. Loveday (the SDSS collaboration), *Contemp. Phys.***43**, 437 (2002); M. Tegmark, M. Blanton, M. Strauss, *et al.*, *Astrophys. J.***606**, 702 (2004); J. Adelman-McCarthy, M. Agueros, S. Allam, *et al.*, *Astrophys. J.Suppl.* **162**, 38 (2004).
- [4] E. Komatsu *et al.* [WMAP Collaboration], arXiv:0803.0547 [astro-ph].
- [5] G. La Vacca, S. A. Bonometto and L. P. L. Colombo, *New Astronomy*, In Press, arXiv:0810.0127 [astro-ph].
- [6] Q. R.Ahmad *et al.*, *Phys. Rev. Lett.***89**, 011301 (2002); S. N.Ahmed *et al.*, *Phys. Rev. Lett.***92**, 181301 (2004).
- [7] K. Eguchi *et al.*, *Phys. Rev. Lett.***90**, 021802h (2003); T. Araki *et al.*, *Phys. Rev. Lett.***94**, 081801 (2005).

- [8] W. W. Allison *et al.*, Phys. Lett.**B449**, 137 (1999); M. Ambrosio *et al.*, Phys. Lett.**B517**, 59 (2001).
- [9] M. H. Ahn *et al.*, Phys. Rev. Lett.**90**, 041801h (2003); D. G. Michael *et al.*, Phys. Rev. Lett.**97**, 191801 (2006).
- [10] S.A. Bonometto & R. Valdarnini, Phys. Lett.A **104**, 369 (1984); R. Valdarnini & S. Bonometto, A&A **146**, 235 (1985); R. Valdarnini & S. Bonometto, Astrophys. J.**299**, L71 (1985); Achilli S., Occhionero F. & Scaramella R., Astrophys. J.**299**, 577 (1985)
- [11] J. Lesgourgues & S. Pastor, Phys. Rept. 429 (2006) 307-379
- [12] Ratra B. & Peebles P.J.E. (1988) PR D**37**, 3406.
- [13] Brax P and Martin J 1999 Phys. Lett.**B468** 40; Brax P and Martin J 2000 Phys. Rev.**D61** 103502
- [14] L. Colombo & M. Gervasi, JCAP **10**, 001 (2006).
- [15] Wetterich C., A&A **301**, 321 (1995); Amendola L., Phys. Rev.**D62**, 043511 (2000).
- [16] L. Amendola & C. Quercellini, Phys. Rev.**D 68**, 023514 (2003); Maccio' A. V., Quercellini C., Mainini R., Amendola L., Bonometto S. A., Phys. Rev.**D69**, 123516 (2004).
- [17] R. Mainini & S. Bonometto, JCAP 0706:020 (2007); Olivares G., Atrio Barandela F. & Pavon D., Phys. Rev.**D 77**, 063513 (2008)
- [18] Damour T., Gibbons G. W. & Gundlach C., 1990, Phys.Rev., L64, 123D Damour T. & Gundlach C., 1991, Phys.Rev., D43, 3873
- [19] L. Amendola, Phys. Rev.**D 60**, 043501 (1999); V. Pettorino and C. Baccigalupi, Phys. Rev.**D 77**, 103003 (2008)
- [20] M. R. Nolta *et al.*, arXiv:0803.0593 [astro-ph]; J. Dunkley *et al.*, arXiv:0803.0586 [astro-ph].
- [21] S. Cole *et al.*, Mon. Not. R. Aston. Soc.**362**, 505 (2005).
- [22] P. Astier *et al.*, A&A **447**, 31 (2006).
- [23] W. L. Freedman *et al.*, Astrophys. J., **553**, 47 (2001).
- [24] S. Burles, K. M. Nollett & M. S. Turner Phys. Rev.**D, 63**, 063512 (2001); R. H. Cyburt, Phys. Rev.**D 70**, 023505 (2004); P. D. Serpicio *et al.*, JCAP, **0412**, 010 (2004).
- [25] A. Lewis & S. Bridle, Phys. Rev.**D, 66**, 103511 (2002).
- [26] A. Lewis, A. Challinor & A. Lasenby, Astrophys. J., **538**, 473 (2000); <http://www.camb.info/>.
- [27] KATRIN collaboration. KATRIN design report 2004. <http://www.wik.fzk.de/katrin/publications/documents/DesignReport2004-12Jan2005.pdf>, 2005.
- [28] J.R. Kristiansen, G. La Vacca, L.P.L. Colombo, R. Mainini, S. A. Bonometto, arXiv:0902.2737 [astro-ph] (2009)